THE JOURNAL OF BIOLOGICAL CHEMISTRY VOL. 291, NO. 48, pp. 25247–25254, November 25, 2016

Transgenic Expression of the Mitochondrial Chaperone TNFR-associated Protein 1 (TRAP1) Accelerates Prostate Cancer Development*[S]

Received for publication, June 28, 2016, and in revised form, October 9, 2016 Published, JBC Papers in Press, October 17, 2016, DOI 10.1074/jbc.M116.745950

Sofia Lisanti[‡§], David S. Garlick[‡], Kelly G. Bryant[‡§], Michele Tavecchio[‡§], Gordon B. Mills[¶], Yiling Lu[¶], Andrew V. Kossenkov[‖], Louise C. Showe[‖], Lucia R. Languino[‡‡], and Dario C. Altieri[‡§1]**

*From the [‡]Prostate Cancer Discovery and Development Program, [§]Tumor Microenvironment and Metastasis Program, [‖]Center for Systems and Computational Biology, and **Molecular and Cellular Oncogenesis Program, The Wistar Institute, Philadelphia, Pennsylvania 19104, the [¶]Department of Systems Biology, University of Texas MD Anderson Cancer Center, Houston, Texas 77030, and the [‡‡]Department of Cancer Biology, Kimmel Cancer Center, Thomas Jefferson University, Philadelphia, Pennsylvania 19107*

Edited by John Denu

Protein homeostasis, or proteostasis, is required for mitochondrial function, but its role in cancer is controversial. Here we show that transgenic mice expressing the mitochondrial chaperone TNFR-associated protein 1 (TRAP1) in the prostate develop epithelial hyperplasia and cellular atypia. When examined on a Pten$^{+/-}$ background, a common alteration in human prostate cancer, TRAP1 transgenic mice showed accelerated incidence of invasive prostatic adenocarcinoma, characterized by increased cell proliferation and reduced apoptosis, *in situ*. Conversely, homozygous deletion of TRAP1 delays prostatic tumorigenesis in Pten$^{+/-}$ mice without affecting hyperplasia or prostatic intraepithelial neoplasia. Global profiling of Pten$^{+/-}$-TRAP1 transgenic mice by RNA sequencing and reverse phase protein array reveals modulation of oncogenic networks of cell proliferation, apoptosis, cell motility, and DNA damage. Mechanistically, reconstitution of Pten$^{+/-}$ prostatic epithelial cells with TRAP1 increases cell proliferation, reduces apoptosis, and promotes cell invasion without changes in mitochondrial bioenergetics. Therefore, TRAP1 is a driver of prostate cancer *in vivo* and an "actionable" therapeutic target.

Mechanisms of protein folding quality control in mitochondria are essential to buffer proteotoxic stress, prevent an unfolded protein response, and promote cellular adaptation to an unfavorable environment (1). Mainly relying on chaperone-directed protein (re)folding (2) or, conversely, proteolytic removal of misfolded or aggregated molecules (3), heightened protein homeostasis, or proteostasis, is critical to maintain mitochondrial function (4).

There is evidence that this pathway is exploited in cancer, as mitochondria of tumor cells contain higher levels of the ATPase-directed chaperone heat shock protein 90 (Hsp90) and its homolog, TNFR-associated protein 1 (TRAP1)[2] (5), compared with normal tissues (6). These molecules preserve the folding of key regulators of oxidative phosphorylation, membrane permeability transition, and redox balance (7). Accordingly, structural requirements of TRAP1 regulation of mitochondrial cell death have been elucidated recently (8). In this context, pharmacologic or genetic interference with Hsp90/TRAP1-directed protein folding causes collapse of multiple mitochondrial functions (7, 9) with suppression of tumor cell proliferation (10, 11), induction of apoptosis (9, 12, 13), and inhibition of cell invasion (14, 15). These data have prompted a model in which mitochondrial proteostasis mediated by Hsp90/TRAP1 is exploited for tumor maintenance (7), including prostate cancer (16), and may provide a therapeutic target (6). Other results, however, have challenged this view and suggested that TRAP1 actually suppresses oxidative phosphorylation to promote glycolysis (17), blocks cell motility (18), and may potentially function as a "tumor suppressor," at least in certain tumors (18).

To resolve these inconsistencies and understand the role of mitochondrial protein folding in disease, we have now generated the first transgenic mouse model with tissue-specific expression of TRAP1 in the prostate. This experimental setting mimics the human disease, as TRAP1 is undetectable or present at low levels in normal prostatic epithelium but becomes abundantly expressed in primary and metastatic prostate cancer (19).

Results

Generation of TRAP1 Transgenic Mice—To test the role of TRAP1 on tumor formation *in vivo*, we generated transgenic (Tg) mice with prostate-specific expression of TRAP1 (6) under the control of the Probasin (Pbsn) promoter. Coinciding with the activity of the Pbsn promoter at sexual maturity, these mice

* This work was supported by National Institutes of Health Grants P01 CA140043 (to D. C. A. and L. R. L.), R01 CA78810 and CA190027 (to D. C. A.), and R01 CA089720 (to L. R. L.), the Office of the Assistant Secretary of Defense for Health Affairs through the Prostate Cancer Research Program under Award W81XWH-13-1-0193 (to D. C. A.), and a Challenge Award from the Prostate Cancer Foundation (to L. R. L. and D. C. A.). The authors declare that they have no conflicts of interest with the contents of this article. The content is solely the responsibility of the authors and does not necessarily represent the official views of the National Institutes of Health.

[S] This article contains supplemental Tables 1 and 2.

[1] To whom correspondence should be addressed: The Wistar Institute, 3601 Spruce St., Philadelphia, PA 19104. Tel.: 215-495-6970; Fax: 215-573-2097; E-mail: daltieri@wistar.org.

[2] The abbreviations used are: TRAP, TNFR-associated protein; Tg, transgenic; Pbsn, Probasin; RPPA, reverse phase protein array; OCR, oxygen consumption rate.

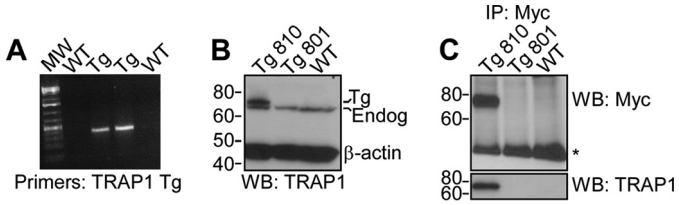

FIGURE 1. **Characterization of TRAP1 transgenic mice.** *A*, total RNA extracted from prostate samples of WT or TRAP1 Tg mice was amplified with primers for TRAP1 by RT-PCR. *MW*, molecular weight. *B*, prostate extracts isolated from WT or two independent TRAP1 Tg lines were analyzed by Western blotting (*WB*). The position of endogenous (*Endog*) or Tg TRAP1 bands is indicated. Only mouse line 810 expresses Tg TRAP1. *C*, prostate extracts isolated from WT or TRAP1 Tg mice were immunoprecipitated (*IP*) with an antibody to Myc and analyzed with an antibody to Myc (*top*) or TRAP1 (*bottom*) by Western blotting. *Asterisk*, not specific. For *B* and *C*, molecular mass markers (in kilodaltons) are indicated.

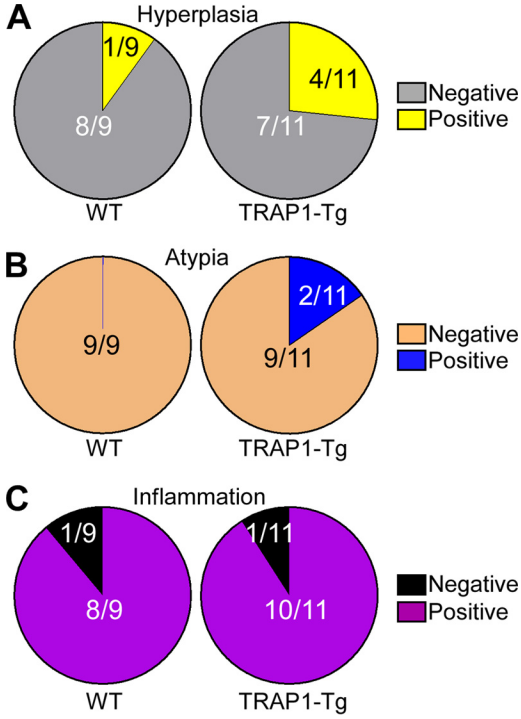

FIGURE 2. **Histopathology of TRAP1 Tg mice.** *A–C*, prostate tissue samples isolated from WT or TRAP1 Tg mice were examined at 12–15 months of age and histologically scored for hyperplasia (*A*), atypia of the prostatic epithelium (*B*), or inflammation (*C*).

expressed Tg TRAP1 mRNA (Fig. 1*A*) and protein (Fig. 1*B*) in isolated prostate tissue extracts. In addition, Myc-tagged Tg TRAP1 immunoprecipitated from prostate extracts reacted with an antibody to TRAP1 (Fig. 1*C*), confirming the identity of the prostate-expressed Tg protein as TRAP1. TRAP1 Tg mice were born viable and fertile and showed no overt phenotype throughout an 18-month observation period. Histologic examination at 12–15 months of age demonstrated that Tg expression of TRAP1 resulted in increased hyperplasia (Fig. 2*A*) and cytologic atypia of the prostatic epithelium (Fig. 2*B*) compared with WT mice. In contrast, prostate inflammation was indistinguishable in WT and TRAP1 Tg mice (Fig. 2*C*). No tumor formation in the prostate was observed in TRAP1 Tg mice or control littermates throughout an 18-month observation period.

Characterization of Pten$^{+/-}$-TRAP1 Tg Mice—To study the effect of TRAP1 on prostate tumorigenesis, we next bred TRAP1 Tg mice with mice heterozygous for the Pten tumor suppressor (20), a common molecular abnormality and driver of prostate cancer in humans (21). Beginning at 6 months of age, Pten$^{+/-}$-TRAP1 Tg mice exhibited increased incidence ($p = 0.04$) of (micro)invasive prostatic adenocarcinoma compared with Pten$^{+/-}$ mice (Fig. 3, *A* and *B*). Tumors in Pten$^{+/-}$-TRAP1 Tg mice were observed in all prostatic lobes (Fig. 3*A*). In reciprocal experiments, we next crossed heterozygous Pten$^{+/-}$ mice with TRAP1 knockout mice (22). Loss of TRAP1 in Pten$^{+/-}$ mice reduced the incidence of prostatic adenocarcinoma compared with TRAP1$^{+/+}$ mice (Fig. 3*C*). This effect was specific for tumor formation, as the incidence of prostate hyperplasia (Fig. 3*D*) or prostatic intraepithelial neoplasia (Fig. 3*E*) was indistinguishable in Pten$^{+/-}$-TRAP1$^{+/+}$ and Pten$^{+/-}$-TRAP1$^{-/-}$ mice. Histologically, early-onset prostate adenocarcinomas formed in Pten$^{+/-}$-TRAP1 Tg mice was associated with reduced apoptosis, as shown by internucleosomal DNA fragmentation (Fig. 4, *A* and *B*), and increased cell proliferation, as shown by Ki67 staining (Fig. 4, *C* and *D*), compared with Pten$^{+/-}$ mice.

Global Profiling of TRAP1 Tg Mice—To better understand the molecular requirements of TRAP1-directed tumorigenesis, we next profiled prostate samples isolated from various Tg mice by RNA sequencing and reverse phase protein array (RPPA). Tg expression of TRAP1 alone did not affect gene expression, as shown by RNA sequencing (Fig. 5*A*). Instead, Pten$^{+/-}$-TRAP1 Tg mice exhibited global transcriptional changes in the prostate with differential up- or down-regulation of 358 genes compared with Pten$^{+/-}$ mice (supplemental Table 1), with 30 genes being differentially expressed at least 10-fold (Fig. 5*A*). Similar results were observed at the protein level by RPPA analysis, where 47 proteins were found to be significantly up-regulated in Pten$^{+/-}$-TRAP1 Tg mice (supplemental Table 2). Regulators of bioenergetics, cytoprotection, angiogenesis, and cell motility were among the top 25 proteins that differed by at least 2-fold in Pten$^{+/-}$-TRAP1 Tg mice compared with control littermates (Fig. 5*B*). In validation studies, prostate samples of Pten$^{+/-}$-TRAP1 Tg mice showed increased expression of anti-apoptotic Bcl2, the stress response chaperone Hsp27, and the metabolic regulator GAPDH (Fig. 5*C*). Bioinformatics analysis of combined RNA sequencing and RPPA data confirmed these results and demonstrated that Tg expression of TRAP1 affected gene networks of apoptosis resistance, cell motility, angiogenesis, DNA damage, and cholesterol/androgen biosynthesis (Fig. 5*D*).

Reconstitution of Pten$^{+/-}$ Prostate Epithelial Cells with TRAP1—To independently validate the TRAP1 phenotype observed *in vivo*, we next reconstituted prostate epithelial cells with TRAP1 cDNA. Experiments with primary prostate epithelial cells isolated from TRAP1 Tg mice were unsuccessful because of the loss of Tg expression in culture (Fig. 6*A*). To overcome this limitation, we transfected Pten$^{+/-}$ P8 prostate epithelial cells with a TRAP1 cDNA (Fig. 6*B*). Consistent with the results *in vivo*, TRAP1-P8 transfectants showed improved cell viability after exposure to the pro-apoptotic stimulant staurosporine compared with control transfectants (Fig. 6*B*) and exhibited reduced caspase-3/7 activity in response to the pro-apoptotic chemotherapeutic agent etoposide (Fig. 6*C*). Similar results were obtained with TRAP1 expression in Pten$^{-/-}$ pros-

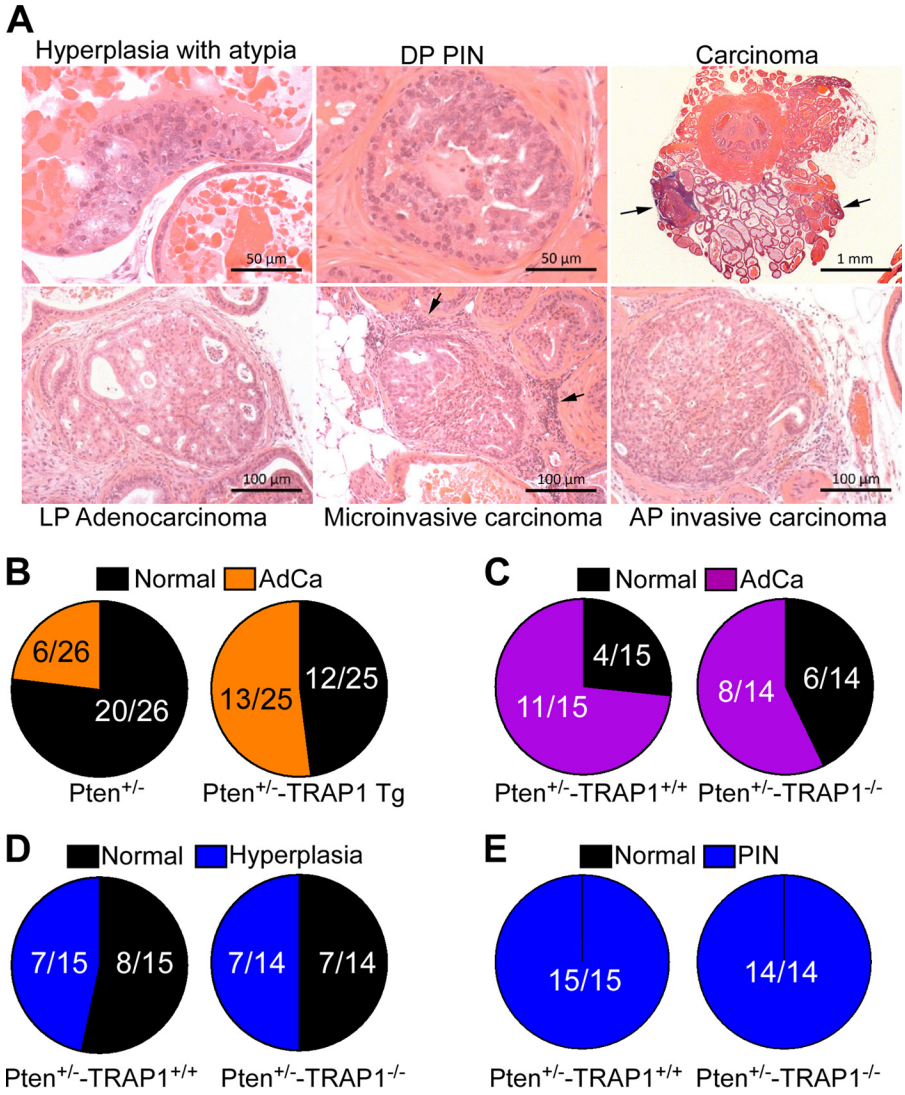

FIGURE 3. **Tg expression of TRAP1 accelerates prostate tumorigenesis.** *A*, prostate tissue sections from Pten$^{+/-}$-TRAP1 Tg mice were analyzed histologically by H&E staining and light microscopy. The individual diagnoses are indicated. Specific pathologies are indicated with *arrows*. *DP*, dorsal prostate; *LP*, lateral prostate; *AP*, anterior prostate; *PIN*, prostatic intraepithelial neoplasia. *B*, quantification of prostatic adenocarcinoma (*AdCa*) in Pten$^{+/-}$ and Pten$^{+/-}$-TRAP1 Tg mice (3–9 months of age). The number of animals examined per condition is indicated. $p = 0.04$. *C–E*, Pten$^{+/-}$-TRAP1$^{+/+}$ or Pten$^{+/-}$-TRAP-1$^{-/-}$ mice were examined histologically for prostate adenocarcinoma (*C*), prostate hyperplasia (*D*), or prostatic intraepithelial neoplasia (*E*). The number of animals examined per condition is indicated.

tate epithelial CapP8 cells (Fig. 6*C*). In addition, TRAP1-P8 transfectants demonstrated increased cell proliferation (Fig. 6*D*) and greater invasion across Matrigel-coated Transwell inserts (Fig. 6*E*). Instead, and at variance with earlier reports (17, 18), TRAP1 overexpression in Pten$^{+/-}$ cells did not affect the ATP/ADP ratio (Fig. 6*F*), oxygen consumption rates (OCR, Fig. 6*G*), or mitochondrial superoxide production (Fig. 6*H*) compared with control transfectants. In these experiments, treatment with the mitochondrial complex I inhibitor rotenone comparably reduced OCR in control or TRAP1 reconstituted P8 cells (Fig. 6*G*), and exposure to the oxidative stimulant H_2O_2 comparably elevated superoxide production in control or TRAP1 transfectants (Fig. 6*H*).

Discussion

In this study, we used genetic manipulations in mice to identify an important role of TRAP1 as an accelerator of prostatic tumorigenesis *in vivo*, cooperating with heterozygous loss of Pten (21) to produce early-onset microinvasive prostate cancer.

Structurally characterized as a mitochondrion-localized Hsp90 chaperone (23), TRAP1 is mostly overexpressed in human cancer compared with normal tissues (6) and has been implicated in tumor cell proliferation (10, 11), apoptosis resistance (9, 12), and metabolic reprogramming (7). Although TRAP1 knockout mice show reduced incidence of age-associated pathologies, including spontaneous tumor formation (22), direct evidence that this pathway is important for tumor growth *in vivo* had remained elusive. Although deletion of other tumor suppressors, for instance SMAD4 (24) or JNK (25), synergizes with loss of Pten to drive invasive prostate cancer, a role of mitochondrial regulator(s) such as TRAP1 in this response has not been explored previously.

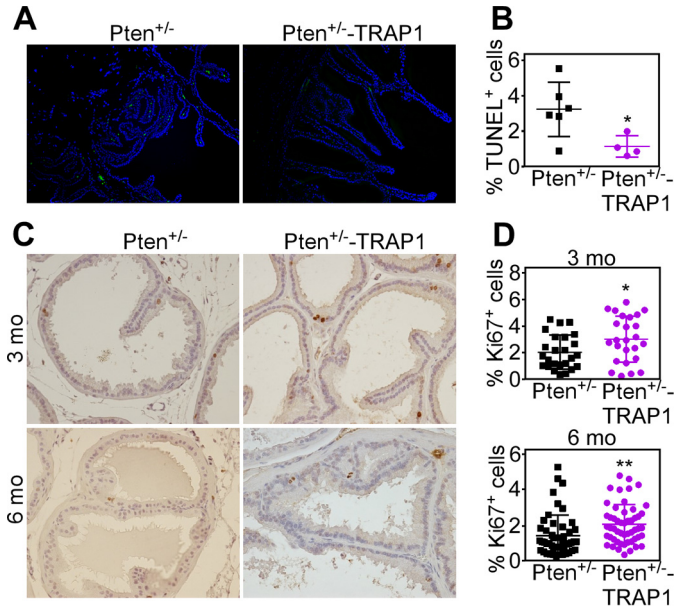

FIGURE 4. **Histopathology of TRAP1 transgenic mice.** *A* and *B*, prostate tissue sections from Pten$^{+/-}$ or Pten$^{+/-}$-TRAP1 Tg mice at 3 months of age were analyzed for apoptosis by TUNEL staining (*A*) with quantification of TUNEL^{+} cells (*B*). *, $p = 0.03$. *C* and *D*, the experimental conditions are as in *A* and *B*, except that prostate tissue sections from Pten$^{+/-}$ or Pten$^{+/-}$-TRAP1 Tg mice at 6 months of age were analyzed for cell proliferation by Ki67 staining (*C*), and the percentage of Ki67^{+} cells at 3 or 6 months (*mo*) of age was quantified (*D*). *, $p = 0.02$; **, $p = 0.005$. Data are mean ± S.D. Each point corresponds to an individual measurement from two (*B*) or four (*C* and *D*) independent mice per genotype.

The oncogenic signal(s) involved in TRAP1 tumorigenesis remain(s) to be fully elucidated. In addition to heightened cell proliferation (10, 11) and inhibition of apoptosis (9, 12) *in vivo*, TRAP1 Tg mice exhibited extensive transcriptional changes, resulting in an angiogenic, pro-invasive, and cytoprotective gene signature. Widespread changes in gene expression were also observed in TRAP1 knockout mice (22) and cell type-specific responses after TRAP1 targeting (26). These data anticipate a potential role of TRAP1-directed proteostasis in mechanisms of mitochondrion-to-nucleus "retrograde" signaling (27), typically activated in response to mitochondrial dynamics (28) or organelle dysfunction (29).

At least in the model of prostate cancer, the results presented here rule out earlier suggestions that TRAP1 may function as a tumor suppressor (18) or inhibitor of mitochondrial respiration (17). Accordingly, TRAP1 reconstitution in Pten$^{+/-}$ P8 prostate epithelial cells did not affect mitochondrial oxygen consumption, ATP production, or reactive oxygen species generation (17). Also contrary to earlier results (18), TRAP1 stimulated epithelial cell invasion, reinforcing a role of this pathway in tumor cell motility and metastatic competence (14).

Altogether, we propose that increased TRAP1 expression in the prostate (19) maintains mitochondrial "fitness" through heightened protein folding quality control (4). The ensuing phenotype of improved bioenergetics (7), ROS buffering (22), and apoptosis resistance (9) may be ideally poised to cooperate with other oncogenic signals, for instance, deregulated Akt activation (30), to accelerate malignant transformation. Conversely, this pathway is "druggable" and may offer new therapeutic opportunities in advanced prostate cancer (16).

Experimental Procedures

Preparation of a TRAP1 Tg Construct—A human TRAP1 cDNA (CDS CCDS27914 Ensemble Genome Database) was amplified from a universal cDNA library using primers CAG GGA TCC ACC ATG GCG CGC GAG CTG (forward) and CAG CTC GAG GTG TCG CTC CAG GGC CTT (reverse) and cloned into the pcDNA^{TM}6/myc-His plasmid (Invitrogen) using BamHI/XhoI restriction sites. A rat Pbsn promoter (−716/+28) identified using the Genomatix database was amplified from commercially available rat genomic DNA (Clontech, catalog no. 636404) using primers CAG GGT ACC ACT TTA TCT TTG GGA TCA AGA CT (forward) and CAG GGA TCC CTG TAG GTA TCT GGA CCT CAC T (reverse). Upon reaching sexual maturity, this promoter sequence specifically drives expression of downstream genes to the prostate (31). The Pbsn insert was cloned into Myc-pcDNA using KpnI/BamHI restriction sites upstream of the TRAP1 cDNA.

Transgene Preparation and Establishment of Founders—The Pbsn-TRAP1 transgene construct was digested from the plasmid backbone using restriction endonucleases KpnI + SexAI + SalI, purified with silica columns, and microinjected into fertilized mouse eggs followed by oviduct implantation in pseudopregnant female mice (B6CBAF1/J, a F1 hybrid resulting from a female C57BL6/J and a male CBA/J), exceptional breeders. Genotyping was carried out using end point PCR with forward primer annealing within the Pbsn sequence (Pbsn-TRAP1 Tg, GCA TCT TGT TCT TAG TCT TTT TCT T) and reverse primer annealing within the TRAP1 first exon sequence (Pbsn-TRAP1 Tg, CAC AGA ATT GGT TTT CCT CCC) performed on genomic DNA (predicted transgene-specific PCR product of 379 bp) isolated from tail snips of the resulting litters. A total of 19 males and 29 females were screened. Of these, one male and four females were found to carry the transgene. Two founder mice were selected for colony propagation (male 801 and female 810). Mating was set with a TRAP1 transgene heterozygous and a WT littermate with generation of a hybrid strain, B6CBAF2/J. Two of the offspring positive at genotyping and obtained from the breeding of founders Tg 801 and Tg 810 were sacrificed at 2 months of age (sexually mature) and examined for transgene expression in the prostate, and one of the positive offspring was established for further studies (Tg line 810).

Generation of Pten$^{+/-}$-TRAP1 Tg Mice—A Pten$^{+/-}$ male mouse (http://www.ncbi.nlm.nih.gov/pubmed/9990064) was used in a breeding pair with a TRAP1 Tg female mouse (line 810). Of the resulting offspring, 25% of the animals were used for further experiments (Pten$^{+/-}$-TRAP1 Tg male mice constituted the experimental group, whereas Pten$^{+/-}$ male mice were used as a control group).

Generation of Pten$^{+/-}$-Trap1$^{-/-}$ Mice—A Pten$^{+/-}$ male mouse (20) was used in a breeding pair with a Trap1$^{-/-}$ (22) female mouse (this strain was obtained by backcrossing Trap1$^{+/-}$ male mice with C57BL/6J female mice 10 times). The resulting Pten$^{+/-}$-Trap1$^{+/-}$ mice were further crossed to obtain Pten$^{+/-}$-Trap1$^{+/+}$ (control mice) and Pten$^{+/-}$-Trap1$^{-/-}$ (experimental mice). The colony was maintained by brother × sister mating.

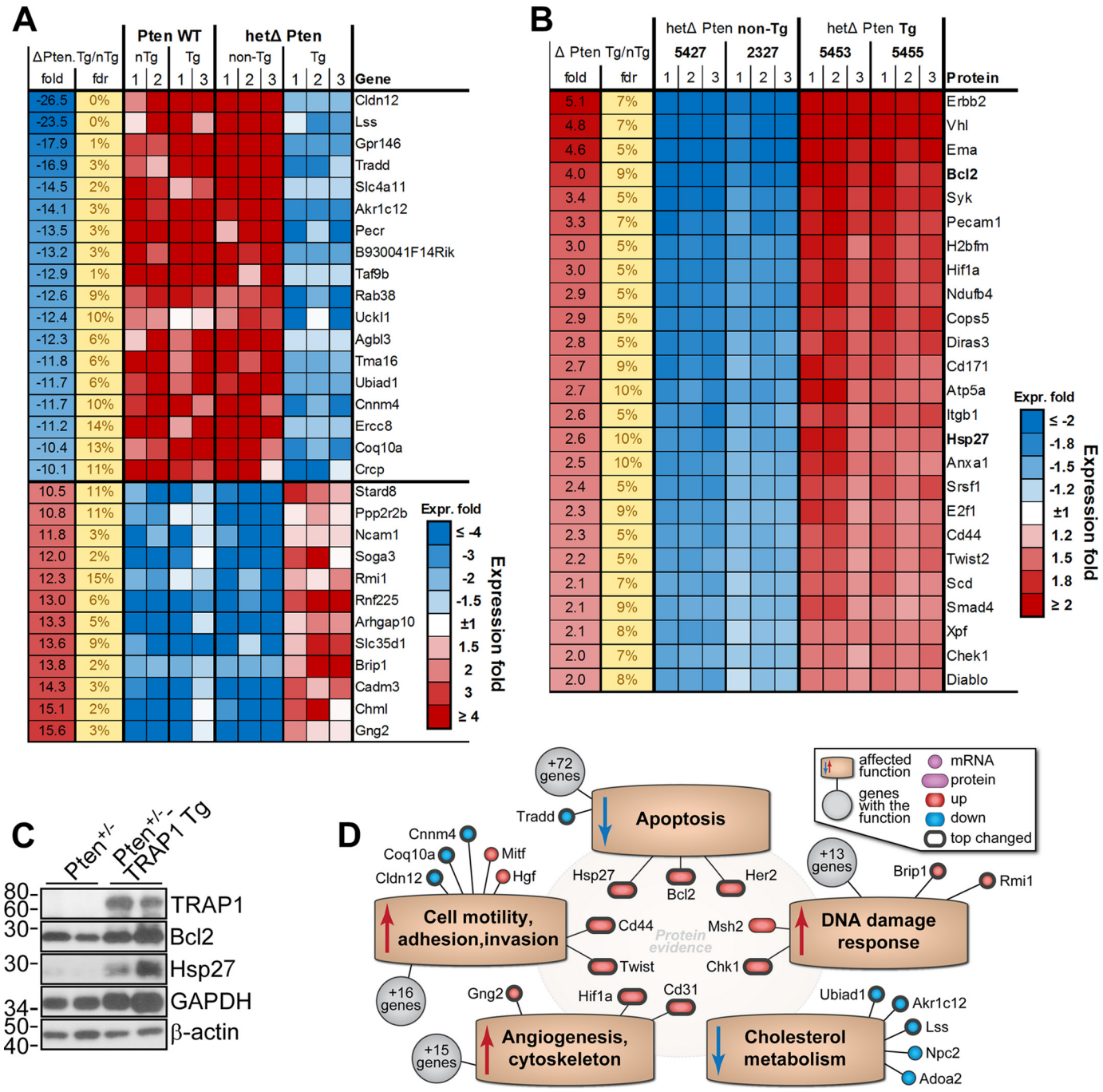

FIGURE 5. **Profiling of TRAP1 Tg mice.** *A*, RNA sequencing. Shown is a heatmap of 30 genes down-regulated (*blue*) or up-regulated (*red*) at least 10-fold in prostate samples isolated from WT or TRAP1 Tg mice or, alternatively, Pten$^{+/-}$ or Pten$^{+/-}$-TRAP1 Tg mice, as identified by RNA sequencing. Only genes with expression of any Pten$^{+/-}$-TRAP1 Tg sample higher or lower than any sample from other groups are shown. *B*, RPPA. Shown is a heatmap of 25 proteins up-regulated at least 2-fold in prostate samples of Pten$^{+/-}$-TRAP1 Tg compared with Pten$^{+/-}$ mice. *C*, prostate samples isolated from Pten$^{+/-}$ or Pten$^{+/-}$-TRAP1 Tg mice were analyzed by Western blotting. Two mice per condition were examined. Molecular mass markers (in kilodaltons) are indicated. *D*, bioinformatics analysis of predicted prostate cancer networks modulated in Pten$^{+/-}$-TRAP1 Tg mice with the most changed genes and proteins highlighted. The impact of transgenic expression of TRAP1 on function is predicted based on Ingenuity Pathway Analysis, activation Z score where available, or overall expression changes of key member genes or directly tested in follow-up experiments.

Immunohistochemistry—Isolated prostate tissue samples from the various mouse cohorts were fixed in formalin and paraffin-embedded. 5-μm sections were deparaffinized with xylene and rehydrated in a graded series of ethanol and water. Tissue samples were analyzed using the *in situ* cell death detection kit (Roche, catalog no. 11684795910) according to the instructions of the manufacturer. Coverslips were mounted on slides with a mounting medium containing DAPI (Antifade Mounting Medium with DAPI, Vectashield, catalog no. H1200) and imaged on a fluorescence microscope. The percentage of TUNEL$^+$ cells was calculated using Nikon NIS Elements software. For Ki67 staining, epitope retrieval was carried out by steaming the slides in 10 mM citrate buffer (pH 6) in a pressure cooker for 10 min on high pressure. After cooling, the slides

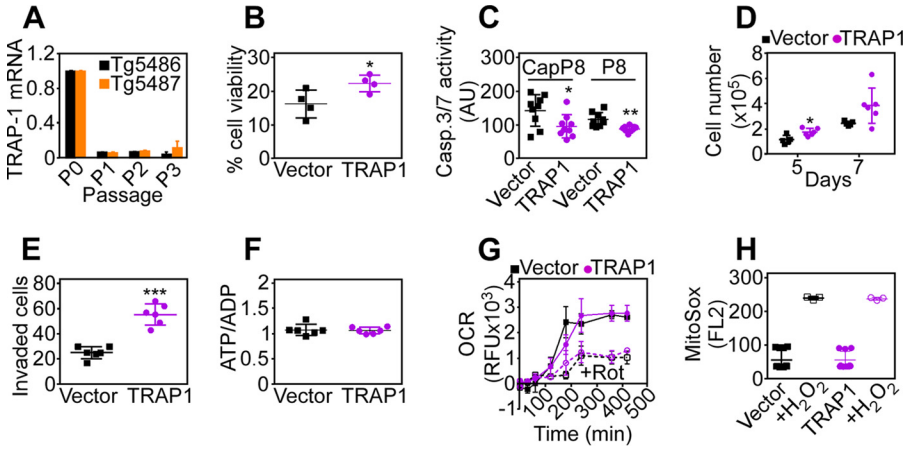

FIGURE 6. **Phenotype of TRAP1 expression in Pten$^{+/-}$ prostate epithelial cells.** *A*, primary prostatic epithelial cells were isolated from TRAP1 Tg mice and analyzed for TRAP1 expression by quantitative PCR at the indicated passages (*P*) in culture. *B*, Pten$^{+/-}$ prostate epithelial P8 cells transfected with vector or TRAP1 cDNA were incubated in the presence of staurosporine (1 μM) and analyzed for cell death by direct cell counting. *C*, Pten$^{-/-}$ prostate epithelial CapP8 cells or P8 cells transfected as in *B* were incubated with etoposide (64 nM) and analyzed for caspase-3/7 activity. *D*—*H*, P8 cells transfected as in *B* were analyzed for cell proliferation by direct cell counting on days 5 and 7 after transfection (*D*), cell invasion across Matrigel-coated inserts (*E*), ATP/ADP ratio (*F*), OCR in the presence or absence of the mitochondrial complex I inhibitor rotenone (*Rot*, 1 μM) (*G*), or mitochondrial superoxide production (*H*). *, $p = 0.01–0.04$; ***, $p < 0.0001$. H_2O_2 was used as a control oxidative stimulus.

were quenched for endogenous peroxidase and blocked for 1 h in 10% goat serum (Vector Labs, S-1000). Slides were incubated with a primary antibody to Ki67 (Abcam, catalog no. ab15580) and diluted 1:100 in 10% goat serum for 16 h at 4 °C. After washes in PBS, the slides were incubated with HRP-conjugated secondary antibody (DAKO Envision+ system HRP-labeled anti-rabbit secondary antibody, catalog no. K4002). Slides were incubated with diaminobenzidine as a chromogen (DAKO Liquid DAB+ substrate chromogen system, catalog no. K3467), counterstained with hematoxylin, and scored by light microscopy. The percentage of Ki67-positive cells was calculated using ImageJ software. Inflammation in the various prostate tissue samples was graded on a 0–4 scoring scale for extent and distribution of inflammatory cell infiltrates as follows: 0 = not present; 1 = minimal; 2 = mild, limited in extent and distribution; 3 = moderate with more extensive involvement of tissue with multifocal to locally extensive distribution; 4 = marked with heavy infiltrates with locally extensive to diffuse distribution.

Western Blotting—Protein lysates from whole cells, whole tissues, or mitochondrial pellets (Thermo Fisher Scientific, catalog no. PI89874) were prepared in the presence of radioimmune precipitation assay buffer (150 mM NaCl, 1.0% Triton X-100, 0.5% sodium deoxycholate, 0.1% SDS, 50 mM Tris (pH 8.0)) with the addition of EDTA-free Halt protease inhibitor (Thermo Scientific, catalog no. 78447) and phosphatase inhibitor mixtures 2 and 3 (Sigma-Aldrich, catalog nos. P5726 and P0044). Equal amounts of protein lysates were separated by SDS-PAGE, transferred onto PVDF membranes, and analyzed with antibodies to TRAP1 (BD Biosciences, catalog no. 612344), BCL-2 (Santa Cruz Biotechnology, catalog no. sc-7382), HSP27 (Cell Signaling Technology, catalog no. 2402), GAPDH (Sigma-Aldrich, catalog no. G8795), β-actin (Sigma-Aldrich, catalog no. A5441), and Myc-Tag (Cell Signaling Technology, catalog no. 2278).

RNA Sequencing—Twelve RNA samples extracted from Tg prostates were first treated with the Invitrogen/Ambion DNA-free kit (catalog no. AM1906) to remove DNA and run on the Agilent 2100 Bioanalyzer for quality assessment. The sequencing libraries were generated using the Lexogen QuantSeq 3′ mRNA sequencing library preparation kit (SKU:015.24) for Illumina sequencing platform-compatible libraries. In these experiments, QuantSeq provides an alternative measure of gene expression to using microarrays. Only one fragment is produced per endogenous transcript, allowing more accurate determination of gene expression values. The KAPA real-time PCR library quantification kit (KK4835) was used to quantify and assess library quality. All 12 libraries were pooled in equal molar amounts and run on an Illumina Nextseq500 using the Mid Output V2 (150 cycles) kit (catalog no. FC-404-2001). Sequences were for 1 × 75 base pairs.

RPPA—Whole prostate lysates from Pten$^{+/-}$ or Pten$^{+/-}$-TRAP1 Tg mice were arrayed on nitrocellulose-coated slides with three technical replicates done for each duplicate sample. Spots were visualized by DAB colorimetric assay, and densities were quantified by Array-Pro analyzer. Linear values were normalized for protein loading before calculation of -fold changes as described previously (32).

Bioinformatics Analysis—For RPPA analysis, the pairwise group comparisons were done using two-sample *t* test applied to technical replicate average values (three technical replicates for each of two samples in two groups), and the Benjamini-Hochberg method was used to correct for multiple testing. Proteins that passed false discovery rate < 15% were considered significantly differentially expressed. Only the proteins that were up-regulated in TRAP1 Tg samples were considered. For RNA sequencing data, raw reads were aligned using the bowtie 2 algorithm (33) against the mm10 genome, and Ensembl transcriptome information was used along with RSEM software (34) to calculate raw read counts for each gene. Two samples were removed as technical outliers based on principal component analysis. Differential expression analysis was done using DESeq2 (35). Genes that passed an FDR threshold of <15% were considered significant. Protein and gene expression data

were visualized as expression heatmaps using Microsoft Excel. Analysis of the gene set for enrichment of biological functions was done using Qiagen Ingenuity® Pathway Analysis software (IPA®). Only results with $p < 0.005$, or with a Z score for predicted activation state calculated by IPA, or where functions of all genes changed in the same direction were studied. A manual literature search was then performed for biological functions of most changed proteins and genes, and only significantly enriched functions with key regulators changed at the protein level (47 proteins) or mRNA level (30 genes with >10-fold) were considered. The final function list was used to generate a model of the most affected processes reflected in the Pten$^{+/-}$-TRAP1 Tg mouse phenotype. The effect on each function was predicted based on either the Ingenuity Pathway Analysis, activation Z score where available, or the behavior of member genes or was directly tested in validation experiments.

Cell Culture—Pten$^{+/-}$ P8 or Pten$^{-/-}$ CapP8 murine prostate epithelial cell lines were obtained from the ATCC (catalog no. ATCC CRL-3031) and cultured in DMEM (ATCC, catalog no 30-2002) with the addition of 10% fetal bovine serum (Gemini Bio Products, catalog no. 100-106), 100 IU/ml penicillin, 100 μg/ml streptomycin, 25 μg/ml bovine pituitary extract (ScienceCell Research Laboratories, catalog no. 0703), 5 μg/ml human recombinant insulin (Sigma-Aldrich, catalog no. I9278), and 6 ng/ml human recombinant epidermal growth factor (STEMCELL Technologies, catalog no. 02633). Cells (1×10^5/60-cm^2 Petri dishes) were transfected with 5 μg of pcDNA His$_6$-Myc-TRAP1 cDNA or vector and 30 μl of Lipofectamine transfection reagent (Thermo Fisher Scientific, catalog no. 18324012) in Opti-MEM I reduced serum medium (Thermo Fisher Scientific, catalog no. 31985070) without antibiotics. After 5 h, cells were washed twice with PBS and cultured in complete medium.

For analysis of apoptosis, P8 cells were transfected with vector or TRAP1 cDNA, treated with the broad-spectrum kinase inhibitor staurosporine (1 μM), and analyzed for cell viability by direct cell counting. In other experiments, P8 or CapP8 cells transfected with vector or TRAP1 cDNA were plated in triplicates (5×10^3) onto 96-well black plates in 100 μl of complete DMEM without phenol red, exposed to etoposide (64 nM), and assayed after 5 h for changes in terminal caspase-3/7 activity using a caspase 3/7 assay kit (eEnzyme, catalog no. CA-C150). Cell invasion experiments across Matrigel-coated inserts (BD Biosciences, catalog no. 354483) were carried out using NIH3T3-conditioned medium in the lower compartment as a chemoattractant, as described previously (14). Control or TRAP1 P8 transfectants were examined for ATP/ADP ratio (BioChain, catalog no. z5030042) and OCRs (Enzo Life Sciences, catalog no. ENZ-51045-K100), as described previously (7), in the presence or absence of the mitochondrial complex I inhibitor rotenone (1 μM). Mitochondrial superoxide production was quantified by fluorescence staining with MitoSOX™ Red (5 μM, 10 min). H_2O_2 was used as a control oxidative stimulus. In some experiments, whole prostates were isolated from male mice between 8 and 12 weeks of age and digested, and the resulting epithelial cells were co-cultured with feeder layers as described previously (36). 5α-Dihydrotestosterone (Sigma-Aldrich, catalog no. D-073) was added at the indicated concentrations for 24 or 48 h before cell harvesting.

Statistical Analysis—Data were analyzed using two-sided unpaired *t* or chi-square tests using a GraphPad software package (Prism 6.0) for Windows. For all experiments, data are expressed as mean ± S.D. with representation of individual replicates from at least two or three independent determinations. $p < 0.05$ was considered statistically significant.

Author Contributions—S. L. and D. C. A. conceived the study. S. L. generated and characterized TRAP1 Tg mice and Pten$^{+/-}$ TRAP1 double Tg mice. S. L. and M. T. performed experiments of tumor cell proliferation, apoptosis, invasion, and bioenergetics. D. S. G. performed mouse pathology. K. G. B. characterized cell proliferation and apoptosis *in vivo*. A. V. K. analyzed bioinformatics data. G. B. M. and Y. L. performed RPPA experiments. S. L., L. C. S., L. R. L., and D. C. A. analyzed data. S. L. and D. C. A. wrote the paper.

Acknowledgments—Support for the core facilities utilized in this study was provided by Cancer Center Support Grants CA010815 to The Wistar Institute and CA016672 to The University of Texas MD Anderson Cancer Center.

References

1. Balch, W. E., Morimoto, R. I., Dillin, A., and Kelly, J. W. (2008) Adapting proteostasis for disease intervention. *Science* **319,** 916–919
2. Taipale, M., Jarosz, D. F., and Lindquist, S. (2010) HSP90 at the hub of protein homeostasis: emerging mechanistic insights. *Nat. Rev. Mol. Cell Biol.* **11,** 515–528
3. Goard, C. A., and Schimmer, A. D. (2014) Mitochondrial matrix proteases as novel therapeutic targets in malignancy. *Oncogene* **33,** 2690–2699
4. Baker, B. M., and Haynes, C. M. (2011) Mitochondrial protein quality control during biogenesis and aging. *Trends Biochem. Sci.* **36,** 254–261
5. Lavery, L. A., Partridge, J. R., Ramelot, T. A., Elnatan, D., Kennedy, M. A., and Agard, D. A. (2014) Structural asymmetry in the closed state of mitochondrial Hsp90 (TRAP1) supports a two-step ATP hydrolysis mechanism. *Mol. Cell* **53,** 330–343
6. Altieri, D. C., Stein, G. S., Lian, J. B., and Languino, L. R. (2012) TRAP-1, the mitochondrial Hsp90. *Biochim. Biophys. Acta* **1823,** 767–773
7. Chae, Y. C., Angelin, A., Lisanti, S., Kossenkov, A. V., Speicher, K. D., Wang, H., Powers, J. F., Tischler, A. S., Pacak, K., Fliedner, S., Michalek, R. D., Karoly, E. D., Wallace, D. C., Languino, L. R., Speicher, D. W., and Altieri, D. C. (2013) Landscape of the mitochondrial Hsp90 metabolome in tumours. *Nat. Commun* **4,** 2139
8. Lebedev, I., Nemajerova, A., Foda, Z. H., Kornaj, M., Tong, M., Moll, U. M., and Seeliger, M. A. (2016) A novel *in vitro* CypD-mediated p53 aggregation assay suggests a model for mitochondrial permeability transition by chaperone systems. *J. Mol. Biol.* **428,** 4154–4167
9. Kang, B. H., Plescia, J., Dohi, T., Rosa, J., Doxsey, S. J., and Altieri, D. C. (2007) Regulation of tumor cell mitochondrial homeostasis by an organelle-specific Hsp90 chaperone network. *Cell* **131,** 257–270
10. Zhang, B., Wang, J., Huang, Z., Wei, P., Liu, Y., Hao, J., Zhao, L., Zhang, F., Tu, Y., and Wei, T. (2015) Aberrantly upregulated TRAP1 is required for tumorigenesis of breast cancer. *Oncotarget* **6,** 44495–44508
11. Agorreta, J., Hu, J., Liu, D., Delia, D., Turley, H., Ferguson, D. J., Iborra, F., Pajares, M. J., Larrayoz, M., Zudaire, I., Pio, R., Montuenga, L. M., Harris, A. L., Gatter, K., and Pezzella, F. (2014) TRAP1 regulates proliferation, mitochondrial function, and has prognostic significance in NSCLC. *Mol. Cancer Res.* **12,** 660–669
12. Chae, Y. C., Caino, M. C., Lisanti, S., Ghosh, J. C., Dohi, T., Danial, N. N., Villanueva, J., Ferrero, S., Vaira, V., Santambrogio, L., Bosari, S., Languino, L. R., Herlyn, M., and Altieri, D. C. (2012) Control of tumor bioenergetics and survival stress signaling by mitochondrial HSP90s. *Cancer Cell* **22,** 331–344

13. Lee, C., Park, H. K., Jeong, H., Lim, J., Lee, A. J., Cheon, K. Y., Kim, C. S., Thomas, A. P., Bae, B., Kim, N. D., Kim, S. H., Suh, P. G., Ryu, J. H., and Kang, B. H. (2015) Development of a mitochondria-targeted Hsp90 inhibitor based on the crystal structures of human TRAP1. *J. Am. Chem. Soc.* **137,** 4358–4367
14. Caino, M. C., Chae, Y. C., Vaira, V., Ferrero, S., Nosotti, M., Martin, N. M., Weeraratna, A., O'Connell, M., Jernigan, D., Fatatis, A., Languino, L. R., Bosari, S., and Altieri, D. C. (2013) Metabolic stress regulates cytoskeletal dynamics and metastasis of cancer cells. *J. Clin. Invest.* **123,** 2907–2920
15. Agliarulo, I., Matassa, D. S., Amoroso, M. R., Maddalena, F., Sisinni, L., Sepe, L., Ferrari, M. C., Arzeni, D., Avolio, R., Paolella, G., Landriscina, M., and Esposito, F. (2015) TRAP1 controls cell migration of cancer cells in metabolic stress conditions: correlations with AKT/p70S6K pathways. *Biochim. Biophys. Acta* **1853,** 2570–2579
16. Kang, B. H., Siegelin, M. D., Plescia, J., Raskett, C. M., Garlick, D. S., Dohi, T., Lian, J. B., Stein, G. S., Languino, L. R., and Altieri, D. C. (2010) Preclinical characterization of mitochondria-targeted small molecule hsp90 inhibitors, gamitrinibs, in advanced prostate cancer. *Clin. Cancer Res.* **16,** 4779–4788
17. Sciacovelli, M., Guzzo, G., Morello, V., Frezza, C., Zheng, L., Nannini, N., Calabrese, F., Laudiero, G., Esposito, F., Landriscina, M., Defilippi, P., Bernardi, P., and Rasola, A. (2013) The mitochondrial chaperone TRAP1 promotes neoplastic growth by inhibiting succinate dehydrogenase. *Cell Metab.* **17,** 988–999
18. Yoshida, S., Tsutsumi, S., Muhlebach, G., Sourbier, C., Lee, M. J., Lee, S., Vartholomaiou, E., Tatokoro, M., Beebe, K., Miyajima, N., Mohney, R. P., Chen, Y., Hasumi, H., Xu, W., Fukushima, H., *et al.* (2013) Molecular chaperone TRAP1 regulates a metabolic switch between mitochondrial respiration and aerobic glycolysis. *Proc. Natl. Acad. Sci. U.S.A.* **110,** E1604–1612
19. Leav, I., Plescia, J., Goel, H. L., Li, J., Jiang, Z., Cohen, R. J., Languino, L. R., and Altieri, D. C. (2010) Cytoprotective mitochondrial chaperone TRAP-1 as a novel molecular target in localized and metastatic prostate cancer. *Am. J. Pathol* **176,** 393–401
20. Podsypanina, K., Ellenson, L. H., Nemes, A., Gu, J., Tamura, M., Yamada, K. M., Cordon-Cardo, C., Catoretti, G., Fisher, P. E., and Parsons, R. (1999) Mutation of Pten/Mmac1 in mice causes neoplasia in multiple organ systems. *Proc. Natl. Acad. Sci. U.S.A.* **96,** 1563–1568
21. Baca, S. C., Prandi, D., Lawrence, M. S., Mosquera, J. M., Romanel, A., Drier, Y., Park, K., Kitabayashi, N., MacDonald, T. Y., Ghandi, M., Van Allen, E., Kryukov, G. V., Sboner, A., Theurillat, J. P., Soong, T. D., *et al.* (2013) Punctuated evolution of prostate cancer genomes. *Cell* **153,** 666–677
22. Lisanti, S., Tavecchio, M., Chae, Y. C., Liu, Q., Brice, A. K., Thakur, M. L., Languino, L. R., and Altieri, D. C. (2014) Deletion of the mitochondrial chaperone TRAP-1 uncovers global reprogramming of metabolic networks. *Cell Rep.* **8,** 671–677
23. Sung, N., Lee, J., Kim, J. H., Chang, C., Joachimiak, A., Lee, S., and Tsai, F. T. (2016) Mitochondrial Hsp90 is a ligand-activated molecular chaperone coupling ATP binding to dimer closure through a coiled-coil intermediate. *Proc. Natl. Acad. Sci. U.S.A.* **113,** 2952–2957
24. Ding, Z., Wu, C. J., Chu, G. C., Xiao, Y., Ho, D., Zhang, J., Perry, S. R., Labrot, E. S., Wu, X., Lis, R., Hoshida, Y., Hiller, D., Hu, B., Jiang, S., Zheng, H., *et al.* (2011) SMAD4-dependent barrier constrains prostate cancer growth and metastatic progression. *Nature* **470,** 269–273
25. Hübner, A., Mulholland, D. J., Standen, C. L., Karasarides, M., Cavanagh-Kyros, J., Barrett, T., Chi, H., Greiner, D. L., Tournier, C., Sawyers, C. L., Flavell, R. A., Wu, H., and Davis, R. J. (2012) JNK and PTEN cooperatively control the development of invasive adenocarcinoma of the prostate. *Proc. Natl. Acad. Sci. U.S.A.* **109,** 12046–12051
26. Kim, H., Yang, J., Kim, M. J., Choi, S., Chung, J. R., Kim, J. M., Yoo, Y. H., Chung, J., and Koh, H. (2016) Tumor necrosis factor receptor-associated protein 1 (TRAP1) mutation and TRAP1 inhibitor gamitrinib-triphenylphosphonium (G-TPP) induce a forkhead box O (FOXO)-dependent cell protective signal from mitochondria. *J. Biol. Chem.* **291,** 1841–1853
27. Kleine, T., and Leister, D. (2016) Retrograde signaling: organelles go networking. *Biochim. Biophys. Acta* **1857,** 1313–1325
28. Khacho, M., Clark, A., Svoboda, D. S., Azzi, J., MacLaurin, J. G., Meghaizel, C., Sesaki, H., Lagace, D. C., Germain, M., Harper, M. E., Park, D. S., and Slack, R. S. (2016) Mitochondrial dynamics impacts stem cell identity and fate decisions by regulating a nuclear transcriptional program. *Cell Stem Cell* **19,** 232–247
29. Cagin, U., Duncan, O. F., Gatt, A. P., Dionne, M. S., Sweeney, S. T., and Bateman, J. M. (2015) Mitochondrial retrograde signaling regulates neuronal function. *Proc. Natl. Acad. Sci. U.S.A.* **112,** E6000–6009
30. Majumder, P. K., Febbo, P. G., Bikoff, R., Berger, R., Xue, Q., McMahon, L. M., Manola, J., Brugarolas, J., McDonnell, T. J., Golub, T. R., Loda, M., Lane, H. A., and Sellers, W. R. (2004) mTOR inhibition reverses Akt-dependent prostate intraepithelial neoplasia through regulation of apoptotic and HIF-1-dependent pathways. *Nat. Med.* **10,** 594–601
31. Yan, Y., Sheppard, P. C., Kasper, S., Lin, L., Hoare, S., Kapoor, A., Dodd, J. G., Duckworth, M. L., and Matusik, R. J. (1997) Large fragment of the probasin promoter targets high levels of transgene expression to the prostate of transgenic mice. *Prostate* **32,** 129–139
32. Zhang, G., Frederick, D. T., Wu, L., Wei, Z., Krepler, C., Srinivasan, S., Chae, Y. C., Xu, X., Choi, H., Dimwamwa, E., Ope, O., Shannan, B., Basu, D., Zhang, D., Guha, M., *et al.* (2016) Targeting mitochondrial biogenesis to overcome drug resistance to MAPK inhibitors. *J. Clin. Invest.* **126,** 1834–1856
33. Langmead, B., and Salzberg, S. L. (2012) Fast gapped-read alignment with Bowtie 2. *Nat. Methods* **9,** 357–359
34. Frezza, C., Zheng, L., Folger, O., Rajagopalan, K. N., MacKenzie, E. D., Jerby, L., Micaroni, M., Chaneton, B., Adam, J., Hedley, A., Kalna, G., Tomlinson, I. P., Pollard, P. J., Watson, D. G., Deberardinis, R. J., *et al.* (2011) Haem oxygenase is synthetically lethal with the tumour suppressor fumarate hydratase. *Nature* **477,** 225–228
35. Love, M. I., Huber, W., and Anders, S. (2014) Moderated estimation of fold change and dispersion for RNA-seq data with DESeq2. *Genome Biol.* **15,** 550
36. Liu, X., Ory, V., Chapman, S., Yuan, H., Albanese, C., Kallakury, B., Timofeeva, O. A., Nealon, C., Dakic, A., Simic, V., Haddad, B. R., Rhim, J. S., Dritschilo, A., Riegel, A., McBride, A., and Schlegel, R. (2012) ROCK inhibitor and feeder cells induce the conditional reprogramming of epithelial cells. *Am. J. Pathol* **180,** 599–607